An Explanation for the Lack of Ion Cyclotron Wave Generation by Pickup Ions at Titan: 1D Hybrid Simulation Results

M. M. Cowee, S. P. Gary, H. Y. Wei, R. L. Tokar, C.T. Russell

Los Alamos National Laboratory

M. M. Cowee, Los Alamos National Laboratory, Los Alamos, NM, 87545, USA. (mcowee@lanl.gov)

Abstract. Titan's dense atmosphere is thought to be an important source of pickup ions in the Saturnian magnetosphere. Cassini spacecraft measurements of the plasmas near Titan show evidence of pickup ions, yet electromagnetic ion cyclotron waves, which are direct indicators of ion pickup, have not yet been detected. Pickup ions and their associated ion cyclotron waves have been observed at Saturn's Extended Neutral Cloud (∼4-10 R_s), as well as at Jupiter's moon, Io, suggesting that the plasma and pickup conditions near Titan may be fundamentally different than these other environments. Using 1D hybrid simulations, we investigate ion cyclotron wave growth for variable conditions in the Titan environment to test which conditions could yield waves with sufficient amplitude to be clearly detected by spacecraft. Results suggest that ion cyclotron waves have not been observed at Titan because their growth time is too long compared to the convection time of background plasma through the interaction region and therefore will not be of sufficient amplitude to be observed by Cassini. Because Titan can be located in either the magnetically noisy Saturnian current sheet or in the magnetically quiet lobe-region, we consider both of these environments in this study.

1. Introduction

Observations by the Voyager spacecraft in 1980 and the Cassini spacecraft from 2004-present have shown a very complex and dynamic interaction between Titan's atmosphere and Saturn's flowing magnetospheric plasma. When Voyager flew by Titan, the magnetometer detected evidence of field-line draping associated with an induced magnetosphere [*Ness et al.*, 1981] and the plasma instrument detected enhanced density and slowing of the flow as the spacecraft neared Titan [*Bridge et al.*, 1981; *Hartle et al.*, 1982]. When Cassini flew by 24 years later, its plasma and magnetic field measurements confirmed those of Voyager and also showed the presence of heavy ions with the energy distribution of pickup ions [*Hartle et al.*, 2006a; *Szego et al.*, 2005]. That Titan is an obstacle to the flowing plasma and a source of mass-loading in Saturn's magnetosphere was not unexpected since Titan is the only moon in the solar system which has a dense atmosphere; however, Cassini observations have shown that the Titan plasma and pickup environment cannot be simply characterized because at Titan's orbital distance of 20 R_s the moon moves in and out of the Saturnian magnetospheric current sheet and can sometimes be in the solar wind [*Bertucci*, 2009; *Rymer et al.*, 2009; *Wei et al.*, 2009].

As Titan orbits around Saturn, its neutral atmosphere is ionized by photoionization, electron impact ionization with the impinging magnetospheric plasma, and charge exchange between ions and neutrals [cf. *Coates*, 2009]. Once ionized, this population of ions is subject to electromagnetic forces which accelerates the ions up to the bulk velocity of the background plasma. Because of this acceleration of a large number of new ions, the background plasma flow slows to conserve the total momentum of the system. The

slowing of the plasma by the presence of Titan while the distant ends of the magnetic flux tubes are carried past Titan cause the magnetic field lines to be bent. Another frequently observable consequence of the ion pickup process is the generation of plasma waves. Because the pickup ions are typically anisotropic they are unstable to the generation of waves which act to scatter the population to a more isotropic configuration in velocity space. Such pickup ion associated plasma waves have been observed in the environments of Venus, Earth, Mars, comets, Jupiter and Saturn [e.g., *Le et al.*, 2001; *Russell et al.*, 2006a; *Tsurutani et al.*, 1989; *Kivelson et al.*, 1996; *Leisner et al.*, 2006].

Direct evidence of pickup ions was seen by the Cassini Plasma Spectrometer (CAPS) during the passes by Titan. From data collected during the Ta pass, *Hartle et al.* [2006a] reported that outside of the Titan interaction region, the plasma was composed of mostly H^+ and H_2^+, with energies equivalent to the bulk plasma flow. Then as Titan entered the interaction region on the anti-Saturn side of Titan, CAPS detected a mix of the background H^+ and H_2^+ as well as higher energy H^+ and H_2^+ pickup ions and heavy pickup ions with $m = 14 - 16$ amu, which were identified as N^+/CH_2^+ and CH_4^+. As Cassini moved further into the interaction region downstream of Titan, pickup N_2^+ was also observed. The energies of these pickup ions were seen to decrease as Cassini moved closer to Titan, consistent with pickup in an increasingly decelerated background plasma flow. The narrowness of the peaks in the ion energy spectra detected on Ta and Tb passes has been attributed as evidence that the pickup ions are in drifting ring configuration [*Szego et al.*, 2005] which is a velocity space distribution typically unstable to waves. Further direct detection of pickup H^+ and H_2^+ has been seen when Titan is in the magnetosheath (M. F. Thomsen, personal communication).

In the inner magnetospheres of Jupiter and Saturn, direct detection of pickup ions [e.g., *Frank and Paterson*, 2000; *Tokar et al.*, 2008] and their associated plasma waves [*Kivelson et al.*, 1996; *Leisner et al.*, 2006] has been seen. In these environments, the generated waves have frequencies close to the cyclotron frequency of the ion species generating them and are called "ion cyclotron waves" (ICW). The amplitudes of the waves are also indicators of the densities of the newborn ions, as larger densities of ions will generate larger amplitude waves [*Huddleston et al.*, 1997]. Thus the characteristics of these waves are proxy indicators of the types of neutrals present and their loss rates. At Jupiter's moon, Io, SO_2^+ and SO^+ cyclotron waves were observed by the Galileo spacecraft, out to distances as far as ∼0.5 jovian radii from the moon [*Russell et al.*, 2003a]. Similarly, in Saturn's Extended Neutral Cloud (∼4-10 R_s), water-group ion cyclotron waves have been observed by Cassini at all azimuths around Saturn [*Russell et al.*, 2006b]. These water-group pickup ions originate from the Extended Neutral Cloud which is sourced primarily by the icy-rings and the venting of water-molecules from the moon, Enceladus [*Johnson et al.*, 2006]. Yet despite more than 60 flybys of the Cassini spacecraft to date, ion cyclotron waves have not been identified even though other signatures of pickup ions are evident at Titan.

To better understand why ion cyclotron waves have not been seen at Titan, we look at differences between the Titan environment and the other giant planet magnetospheric environments where pickup ion generated waves are observed. We then carry out 1D hybrid simulations of wave growth for variable plasma and pickup conditions in the Titan environment. We explore several possibilities for the lack of ion cyclotron wave detection including: (1) the pickup ion population at Titan is simply not unstable to wave growth,

(2) the population is unstable to waves other than the ion cyclotron wave, (3) ion cyclotron waves are being generated but the spacecraft is not able to detect them. This paper is organized as follows: section 2 discusses the ion pickup environments and observed wave properties at Io and the extended neutral cloud compared to the Titan environment; section 3 describes the hybrid simulation technique involved and the simulation setup; section 4 discusses the results; and section 5 provides a summary.

2. Comparison of the Environments at Io, the Extended Neutral Cloud and Titan

At Jupiter's moon Io (5.9 R_j), clear signatures of ICW were detected by the Galileo spacecraft on its passes by the moon during 1995-2001 [e.g. *Kivelson*, 1996; *Russell and Kivelson*, 2000, 2001; *Russell et al.*, 2003b]. Waves were left-hand polarized, typically propagated within ∼20 degrees of B_0 and were primarily at the gyrofrequencies of SO^+ ($m = 48$) and SO_2^+ ($m = 64$), which are the dominant neutral species in Io's atmosphere, but minority ion species in the plasma [*Frank et al.*, 1996]. In the Io plasma torus SO^+ and SO_2^+ dissociate within hours and so a thermalized background of these species does not exist there [*Warnecke et al.*, 1997]. As such, the waves generated by newborn SO^+ and SO_2^+ can grow relatively undamped by the background plasma. Conversely, waves generated by S^+ ($m = 32$) and O^+ ($m = 16$), which are the dominant background species at Io were also occasionally observed, since only sufficiently high densities of these pickup ions could generate waves strong enough to overcome the damping background.

At Saturn's Extended Neutral Cloud (∼4-10 R_s) clear signatures of ICW were detected by the Cassini spacecraft on its many passes during 2004-present [*Leisner et al.*, 2006; *Russell et al.*, 2006b]. The waves were left-hand polarized, typically propagated within

111 $\sim$20 degrees of B_0 and were primarily at the gyrofrequencies of water-group ions ($m \sim 17$)
112 which is consistent with the neutral cloud's source being the icy-rings and the jets of water-
113 vapor coming off Enceladus (4.9 R_s). There was additional ion cyclotron wave power at
114 the gyrofrequencies of heavier ions suspected to be O_2^+ ($m = 32$). Since the composition of
115 both the pickup and background ion components are water-group, the pickup ion densities
116 must be sufficient to generate waves strong enough to overcome the damping background.
117 Since the Extended Neutral Cloud encircles Saturn, ion pickup and ICW generation occurs
118 at all azimuths regardless of the location of Enceladus within the Cloud. Additionally,
119 Cassini's excellent spatial coverage of the region showed that waves extended above and
120 below the equatorial plane a distance of $\sim$0.5 R_s.

121 Magnetometer observations at Titan, however, have shown no evidence of coherent ion
122 cyclotron waves like those seen in these other two environments (Figure 1). At frequencies
123 near the heavy ion gyrofrequencies (i.e. CH_4^+ and N_2^+), the wave power spectral density
124 typically shows no significant power enhancement and analysis of the waves near these
125 gyrofrequencies shows no consistent features: waves may be either left- or right-handed,
126 with elliptical to linear polarization, and propagation angles from field-aligned to quite
127 oblique. Figure 2 shows examples of the observed wave spectra during the (left panel) T21
128 and (right panel) T23 passes by Titan when the moon was located in the southern lobe and
129 current sheet of the Saturnian magnetosphere, respectively. The left panel shows what is
130 typically seen at Titan: no enhanced wave power near the gyrofrequencies of the expected
131 pickup ion species. The right panel shows the best example of ion-cyclotron-like activity
132 observed so far. There is slightly enhanced power near the gyro-frequency of $m = 16$
133 ions and the wave analysis indicates the waves are mostly left-hand elliptically polarized

(ellipticity roughly -0.6) and propagate at a large angle to the field (propagation angle roughly 60^o). Given that this left-handed wave power is only slightly above the noise level and that the wave analysis does not show definitive ion cyclotron-like characteristics (near-circular polarization, near-parallel propagation) we cannot identify these as ion cyclotron waves.

While Titan can be thought of as analogous to these other environments in that it is a source of neutrals within these giant planet magnetospheres, there are some very important differences. Firstly, both Io and the Extended Neutral Cloud are located in the planets' inner magnetospheres where the magnetic field is roughly perpendicular to the corotating background plasma, so the nominal pickup angle, α, does not vary substantially and can be considered roughly 90^o. Figure 3 shows a schematic of ion pickup at Io, where the newborn ions gyrate around the magnetic field and are accelerated in the perpendicular direction by the corotation electric field. The resulting pickup ion distributions are "ring"-shaped in velocity space, and will scatter over time on the generated ICW to a more isotropic configuration. Conversely at Titan ($\sim$20 R_s), the orientation of the ambient magnetic field to the background plasma can vary substantially as Titan moves in and out of the Saturnian current sheet, and sometimes exits the magnetosphere into the solar wind. Here, the magnetic field orientation can vary significantly [*Bertucci*, 2009], and so the pickup angle could be significantly off from 90^o which suggests that conditions may sometimes better resemble ion pickup in a solar wind environment (like that at comets, Mars, or Venus) than that of the near-perpendicular pickup environment of the Jupiter or Saturn's inner magnetospheres.

That Titan can be located in a magnetospheric current sheet while Io and the Extended Neutral Cloud cannot is also an important consideration because of the ambient magnetic field noise level. From the magnetometer observations, the ambient magnetic noise level when Titan was in the current sheet was $\delta B_{noise}/B_0 \sim 0.2$, which is approximately equal to the peak ICW amplitudes observed at Io. At the Extended Neutral Cloud, the ambient magnetic field noise level was so quiet ($\delta B_{noise}/B_0 \sim 0.0001$) that ICW peak amplitudes of $\delta B/B_0 \sim 0.01$ could easily be observed. Thus it is questionable whether the waves observed at the Extended Neutral Cloud, or even at Io, could even be detected in the magnetically noisy Titan environment.

The differences between the inner and outer magnetospheric plasma and field environments is important for the different time and spatial scales involved in the ion pickup and wave generation process. The ambient magnetic field strength at Titan is ∼6 nT [*Backes et al.*, 2005], while at Io it is ∼1800 nT [*Kivelson*, 1996] and in the Extended Neutral Cloud at Enceladus' orbit it is ∼325 nT [*Khurana et al.*, 2007]. The background plasma flow velocity at Titan is 110 km/s [*Hartle et al.*, 2006a] (below the corotation velocity of ∼200 km/s), while it is nearly corotating at Io at 74 km/s [*Frank et al.*, 1996] and at Enceladus' orbit at 39 km/s [*Tokar et al.*, 2006]. Titan's orbital velocity is 6 km/s, Io's is 17 km/s, and Keplerian velocity at Enceladus's orbital distance is 13 km/s. Thus the pickup velocities (for $\alpha = 90^o$) for Titan, Io and the Extended Neutral Cloud at Enceladus' orbit are 100 km/s, 57 km/s, and 26 km/s, respectively. The gyroperiod and gyroradius of the dominant ICW-generating pickup ion species at Io is 2.3 s and 21 km (SO_2^+) and at Enceladus' orbit is 3.7s and 15 km (H_2O^+). Given that these gyroradii are much smaller than the radius of Io (1815 km) or the scale height of the Extended Neutral

Cloud ($\sim$0.5 R_s), finite gyroradius effects can be neglected and the pickup ion populations can be assumed gyrotropic. The convection time of the plasma through the ion pickup region in these two environments is also much longer than ten gyroperiods, so waves have time to grow to saturation.

At Titan, the gyroperiods and gyroradii of the expected primary pickup ions are 10.9 s and 174 km for H^+, 21.9 s and 348 km for H_2^+, 175 s and 2786 km for CH_4^+, and 306 s and 4875 km for N_2^+. In this case, the heavy ion gyroradii are of order or larger than the radius of Titan (2575 km), indicating that finite gyroradius effects are important and the pickup ion population may not be gyrotropic [*Ledvina et al.*, 2004; *Hartle et al.*, 2006b]. Additionally, the convection time of the plasma through the pickup region will be short compared to gyroperiod of the heavy ions, suggesting that the waves will not have sufficient time to grow to saturation. For example, if the pickup region is presumed to extend from 4 R_T upstream of Titan to 4 R_T downstream, then a convecting parcel of plasma moving at 100 km/s relative to Titan can traverse the region in 206 s, which is only slightly longer than one CH_4^+ gyroperiod.

How the growth of ICW is affected by some of these possible differences between the Titan and Io/Extended Neutral Cloud environments can be tested via simulations of varying plasma and pickup conditions. For this study, we focus on the most unstable conditions for ICW growth at Titan, where the ambient magnetic field is perpendicular to the background plasma flow ($\alpha = 90$). For simplicity we also consider the pickup ion population to be gyrotropic. Specific methodology and parameters for our simulation study will be described next.

3. Methodology

To simulate the necessary wave-particle interactions, we use a hybrid technique which considers ions kinetically and electrons as an inertialess fluid [*Winske and Omidi*, 1992]. This simulation code has been used in the past to reproduce the ion cyclotron waves generated by pickup ions at Io and Saturn's Extended Neutral Cloud [*Cowee et al.*, 2006, 2007a, b, 2008, 2007b], as well as near comets [e.g., *Omidi and Winske*, 1986; *Gary et al.*, 1989; *Gary and Sinha*, 1989]. The simulation is one-dimensional in space, but maintains fields and velocities in all three dimensions. Electromagnetic fields are calculated from the ion densities and currents collected on an imposed spatial grid. We consider the plasma to be composed of multiple singly-charged ion components, j, which are either newborn pickup ions or maxwellian background.

For the Titan environment, we consider the background plasma to be homogenous and uniform and composed of H^+ and H_2^+, each with densities $n_j = 0.25$ ions/cc and $T_{\parallel j} = T_{\perp j} = 200$ eV. The pickup ion component is considered to have $m = 16$ which could be CH_4^+ from Titan's atmosphere or water-group neutrals originating from the Extended Neutral Cloud which have been transported out to Titan's orbit and ionized [*Rymer et al.*, 2009]. The pickup ions start with zero density at $t = 0$ and are then injected into the simulation at a constant rate, L, with a constant pickup velocity randomly chosen from a perpendicular cold ring distribution with $T_\parallel \sim 0$ and $T_\perp = 1/2 m_j v_p^2/k_B$ where v_p is the pickup velocity. The pickup velocity is varied between 40 km/s and 100 km/s, where 100 km/s is the nominal pickup velocity (i.e. distances greater than $\sim$2 R_T) and the lower values are representative of ion pickup close to Titan where the flowing magnetospheric plasma has become slowed. The background magnetic field is considered constant and

uniform during the run, with $\mathbf{B}_0 = 6$ nT. These parameters were chosen to be generally representative of the Titan environment when it is within Saturn's magnetosphere and are not meant to reproduce any specific spacecraft measurements.

Injection of pickup ions occurs over a limited region of the simulation box for a limited interval of time, to approximate the size of the mass-loading region and residence time of a parcel of plasma convected through that region as illustrated in Figure 4. This schematic shows that the simulation box is considered to move with the background plasma as it flows past Titan, becoming mass-loaded over time. The mass-loading region is taken as a cylinder of radius 4 R_T, extending from 4 R_T upstream to 4 R_T downstream of Titan. The simulation axis, z, is aligned with the magnetic field because the instability has maximum growth at parallel propagation. The simulation box size is 2000 c/ω_{pi} (250 R_T) which is much larger than the 8 R_T diameter of the mass-loading cylinder, so that waves may grow and propagate out of the region. The system box has 2048 grid cells, with 40000 superparticles per cell. Periodic boundary conditions are imposed but the simulations are stopped before the waves can propagate out one end of the box and into the other side. Injection starts at $t = 0$ and continues over the next 206 s (until $\Omega_i t = 7.4$), which is the time necessary for the simulation box to convect a distance 8 R_T at the nominal 100 km/s flow velocity. Additionally, we initialize the superparticles symmetrically in z and vz to strictly enforce the requirement of zero net current across the simulation box. This causes the waves to grow in a symmetrical fashion with respect to the center of the simulation box.

The simulation input parameters for the runs are given in Table 1. Simulation plasma parameters are defined as follows: plasma frequency is $\omega_{pi}^2 = 4\pi n_o e_i^2/m_i$; gyrofrequency

is $\Omega_i = e_i B_0/(m_i c)$; inertial length is c/ω_{pi}, Alfven speed is $v_A = B_0/\sqrt{\mu_0 n_0 m_p}$; parallel and perpendicular temperatures are $T_{\|j} = 1/2 m_j v_{\|j}^2/k_B$ and $T_{\perp j} = 1/2 m_j v_{\perp j}^2/k_B$; plasma beta is $\beta_j = 2\mu_0 n_0 T_{\|j}/B_0^2$; anisotropy is $A_j = T_{\perp j}/T_{\|j}$. Results are given in terms of the normalized simulation parameters where $c/\omega_{pi} = 322$ km, $v_A = 185$ km/s and $\Omega_i^{-1}/(2\pi) = 175$ s (timescale is normalized to $m = 16$ ion inverse gyrofrequency).

4. Results and Discussion

We first show simulation results for the run with the nominal pickup velocity of $v_p = 100$ km/s and $L = 0.005$ ions/cc/s. Figures 5-7 shows that wave growth and scattering of pickup ions to a more isotropic configuration occurs for these simulation input parameters. The time history of the average fluctuating magnetic field energy density in the injection region shown in Figure 5. The waves exhibit an exponential growth phase and show saturation around $\Omega_i t = 10$. We note that saturation of the instability shortly after pickup ion injection ceases at $\Omega_i t = 7.4$ is coincidental. By $\Omega_i t = 7.4$ the instability had already begun to saturate and so the continued injection of new ions, as was tested in another simulation (not shown), did not yield continued linear growth. In Figure 6, which shows the B_y component of the magnetic fields along the simulation axis at four times during the run, the growth of the waves within the injection region (-4 to $+4$ R_T) and their eventual propagation out of it is clearly seen. At each successive output time, we see the wave amplitude is larger and that the waves have propagated further out of the injection region. We also see that around $\Omega_i t = 5$ the waves have a wavelength of the order of the Titan radius and that they are propagating both parallel and anti-parallel to $\mathbf{B}_0$. Over time, the wavelength increases, consistent with the inverse cascade process predicted for this type of instability [e.g., *Gary et al.*, 1986; *Gary and Winske*, 1993].

The scattering of the pickup ions by the waves is seen in the velocity space distributions at four times during the run shown in Figure 7. The ring distribution is clearly seen in Figure 7 (top), and spreads in both the perpendicular and parallel directions over time. By $\Omega_i t = 10$ the ring has scattered such that it is no longer easily identifiable; the anisotropy of the ring component at this time has been reduced to $T_\perp/T_{||} \sim 1.2$. Similarly, in Figure 7 (bottom), the pickup ions are seen to pitch angle scatter, reducing their perpendicular energy and increasing their parallel energy, thereby reducing the anisotropy of the population. The background ions are also slightly heated by the waves (not shown).

To predict the spectral characteristics of the ion cyclotron waves as would be observed by spacecraft, we consider the growing waves in a reference frame which is essentially fixed with respect to Titan where the ion pickup conditions are uniform throughout the region. For example, if the spacecraft were sitting at a fixed location 2 R_T downstream of Titan (i.e. Figure 4), it would observe a continuously propagating set of waves with the characteristics equivalent to those in the simulation at $\Omega_i t = 5.5$. Since our simulation takes place in a reference frame that is convecting past Titan rather than stationary with respect to it, we carry out a test simulation in the stationary reference frame with continuous injection of pickup ions throughout the simulation box to better approximate the continuously produced growing waves which would be observed. This is not strictly accurate since the spacecraft is not fixed with respect to the Titan interaction, but moves through it with some velocity, but we believe it is a better reference frame for determining the observed wave spectrum than the bulk plasma frame. Figure 8 shows the simulated wave spectra from the test run, which indicates wave power at a range of wavenumbers between $kc/\omega_{pi} \sim 0.5 - 3$, with peak power at $kc/\omega_{pi} \sim 0.2$ with frequency just below the

$m = 16$ ion cyclotron frequency. These results agree with linear theory for a warm ring distribution (Figure 10) which shows growth over a range of wavenumbers with maximum growth near $kc/\omega_{pi} \sim 0.2$ and frequency just below the ion cyclotron frequency. The simulated wave power spectral density shown in Figure 9 clearly indicates peak wave power below the $m = 16$ ion gyrofrequency. When compared to the Cassini observations in Figure 2, we see that there is no PSD peak above the noise level, and that the simulated PSD peak may not be high enough to be observed there.

We note that the maximum average amplitude of the waves in the injection region during the run is $\delta B/B_0 = 0.93$ at $\Omega_i t = 10.2$ which is much higher than the magnetic noise level at Titan, suggesting that such a large amplitude wave could be observed there; however, consideration of the growth times of the waves versus convection time of the plasma by Titan indicates that the waves would not have time to reach these saturated amplitudes by the time they are observed by Cassini. If Cassini is sitting at 2 R_T downstream of Titan, the convection time through our schematic mass-loading region (Figure 4) to the spacecraft would be equivalent to the simulation time at $\Omega_i t = 5.5$. At this time, the simulated waves have an average amplitude in the injection region of $\delta B/B_0 = 0.17$, which is just below the noise level. We note that the results do not indicate that if the spacecraft was further downstream it would be able to observe the waves; although the wave levels remain high in the simulation after growth, in reality the waves will be disrupted by turbulence in the Titan wake and so are unlikely to ever be observed by spacecraft. From this schematic view, we find that the growing wave amplitudes and not the saturated wave amplitudes that should be compared with the ambient magnetic noise level.

Next, we carried out simulations and compared the average wave amplitudes in the injection region at $\Omega_i t = 5.5$ for the run parameters listed in Table 1. We have chosen the standard comparison time of $\Omega_i t = 5.5$ for simplicity despite the fact that the different pickup velocities imply a different flow velocity and subsequently a different transit time through the mass loading region. We presume in this case that the nominal background flow velocity of 100 km/s is maintained for most of the time the plasma parcel is in the mass loading region, and we use the decelerated pickup velocities of 70 km/s and 40 km/s as indicators of the maximum wave amplitudes which could be generated by these less energetic pickup ions. The results, shown in Figure 11, indicate that there are a range of pickup velocities and injection rates which can yield wave amplitudes below the magnetic noise level in the current sheet (dark gray dashed line) and lobe (light gray dashed line). Wave amplitudes below $\delta B/B0 = 0.2$ are obtained for v_p = 100, 70 and 40 km/s for 0.005, 0.013 and 0.108 ions/cc/s, respectively. Similarly, wave amplitudes below $\delta B/B0 = 0.01$ are obtained for the three pickup velocities for 0.0007, 0.001, and 0.004 ions/cc/s, respectively. If we assume a cylindrical mass loading region with radius 4 RT and length 8 RT (volume of 6.8658x10^{27} cc), these injection rates are equivalent to total mass loading rates of 3.4x10^{25}, 8.9x10^{25}, and 7.4x10^{26} ions/s when Titan is in the current sheet and 4.8x10^{24}, 6.9x10^{24}, 2.7x10^{25} ions/s when Titan is in the lobe region for the three pickup velocities, respectively. These rates are in agreement with estimates of heavy ion mass loading rates from global simulation models of 10^{25}-10^{26} ions/s [*Sillanpaa et al.*, 2006; *Simon et al.*, 2007; *Modolo and Chanteur*, 2008].

As was mentioned in section 2, there are other considerations in the growth of ICW that have not been taken into account in our simulations. For example, we have considered

only perpendicular pickup ($\alpha = 90^o$) but the magnetic field and plasma flow conditions at Titan are not uniform as they are at Io or in the Extended Neutral Cloud. It is possible that a variety of pickup angles will exist at Titan, and that the pickup ions will have substantial drift velocities parallel to the magnetic field. Considering pickup ion instabilities in the superAlfvenic solar wind, as is appropriate at comets, an initially cold pickup ion component may be unstable both to ion/ion beam instabilities at $\alpha = 0$ relatively close to the Sun and to ion ring instabilities at $\alpha = 90^o$ in the outer heliosphere [*Gary and Madland*, 1988]; however, because the threshold condition of the former instabilities require $v_{||,beam}/v_A > 1$ [*Gary et al.*, 1985], whereas the latter mode may grow even if $v_p/v_A < 1$, the ion/ion beam instability is unlikely to contribute to fluctuation growth in subAlfvenic magnetospheric environments. To test whether pickup at off-90^o angles could be generating waves other than ICW at Titan we performed test stimulations with $v_p = 100$ km/s and $\alpha = 0^o$, 30^o, and 60^o. The results indicate that at all $\alpha < 90$, the dominant source of free energy is the temperature anisotropy of the ring and not the parallel drift velocity. At $\alpha = 0^o$, where the parallel drift velocity is maximized at $\sim 0.5 v_A$, there is insufficient free energy in the beam to drive instability. At the other pickup angles tested, the generated waves are left-hand ion cyclotron waves that have been Doppler shifted from the cyclotron frequency because of the parallel drift velocity. Figure 12 shows the wave PSD for $\alpha = 30^o$, which shows the peak power Doppler shifted to higher frequencies than in Figure 9.

Other pickup ions at Titan include the heavier mass N_2^+ and the lighter mass H^+ and H_2^+. Simulations with N_2^+ pickup ions show that the N_2^+ ion cyclotron waves can grow, but not on the timescales necessary. The gyroperiod of N_2^+ is 306 s, which means that the

newborn N_2^+ would not execute a full cycloid in the time it takes the background plasma to convect past Titan, and simulation show only the very beginnings of wave growth in this short time (not shown). For H^+ and H_2^+, whose gyroperiods are 11 and 22 seconds, respectively, growth time is not an issue. For ion cyclotron waves generated by these ions, the background thermalized component of H^+ and H_2^+ will efficiently damp the waves. Simulation results (not shown) indicate that in order for waves to grow to observable amplitudes the pickup H^+ and H_2^+ density must build up to at least $\sim$6 times the background H^+ and H_2^+ density. Since a background plasma at Titan that is predominantly pickup ions is not supported by either observations or modeling, we can conclude that H^+ and H_2^+ ion cyclotron waves are unlikely to be generated at Titan.

5. Conclusions

We have carried out the first simulations of pickup ions and their associated wave growth in a Titan-like environment. The results indicate that even under ideal wave growth conditions at Titan (uniform field and flow conditions, $\alpha = 90^o$), ion cyclotron waves are not likely to be observed. For the currently estimated heavy ion pickup rates at Titan, the simulations show that ion cyclotron waves can grow, but their growth time is an impediment to their observability by spacecraft. For CH_4^+ pickup ions, growth and saturation of the waves occurs within several gyroperiods, which is roughly equivalent to the time it takes the mass-loaded plasma to move from upstream to downstream of Titan where a spacecraft might observe the waves. As such, if the spacecraft were to see them, they would be low amplitude growing waves rather than the higher amplitude saturated waves and may not be identifiable over the ambient magnetic noise level at Titan. This does not suggest that higher amplitude waves could be detected further downstream, as

the turbulence in the wake region is likely to disrupt the waves and scatter the pickup ions. For lower pickup rates, the waves may not exhibit any appreciable growth by the time they are convected to the spacecraft and so would not be clearly observed. For N_2^+ pickup ions, whose gyroperiod is even longer than CH_4^+, the generated waves do not show growth within the transit time of the plasma through the mass-loading region. For H^+ or H_2^+ pickup ions, growth time is not an issue but the waves are damped by the H^+ and H_2^+ thermal background.

If we assume the ion cyclotron waves are growing but are below the ambient noise level of $\delta B/B_0 = 0.2$ when Titan is in the current sheet and $\delta B/B_0 = 0.01$ when Titan is in the lobes, then we can estimate the possible ion pickup rates at Titan from the simulated wave amplitudes at $\Omega_i t = 5.5$, when the spacecraft could have observed them. For CH_4^+ pickup ions with pickup velocity 40, 70, and 100 km/s, respectively, we find that the pickup rates should be at most $\sim$ 0.005, 0.013 and 0.108 ions/cc/s in the plasma sheet and 0.0007, 0.001, and 0.004 ions/cc/s in the lobes. If we assume a cylindrical mass loading region with radius 4 RT and length 8 RT, these injection rates are equivalent to total mass loading rates of $3.4\text{x}10^{25}$ - $7.4\text{x}10^{26}$ ions/s when Titan is in the current sheet and $4.8\text{x}10^{24}$ - $2.7\text{x}10^{25}$ ions/s when Titan is in the lobe region. These rates are in agreement with the heavy ion mass loading rates of 10^{25} - 10^{26} ions/s estimated from global simulation models of the Titan interaction [*Sillanpaa et al.*, 2006; *Simon et al.*, 2007; *Modolo and Chanteur*, 2008]. We note that while these simulation results imply that ion cyclotron waves are at the cusp of observability at Titan this is not necessarily the case since we have carried out these simulations with a 1D simulation. In such a system, wave energy is restricted to only one direction of propagation; however, in a 2D or 3D simulation the wave energy

can be spread over a wider range of angles and so the wave amplitudes are likely to be lower.

If the ion cyclotron waves are growing, then they could be actively scattering the pickup ions to a more isotropic configuration in velocity space within several gyroperiods, even if the wave amplitudes are below the ambient magnetic noise level. Simulation results show that the pickup ion ring with $T_\perp \sim 800$ eV is still clearly identifiable in velocity space at $\Omega_i t = 5$, but has scattered to near isotropy with a $T_\perp \sim T_{||} \sim 500$ eV by $\Omega_i t = 10$.

While this study is focused on $\alpha = 90^o$, which yields the most anisotropic pickup ion distributions, the pickup angle at Titan could vary substantially away from 90^o. Simulations for $\alpha = 0^o$, 30^o, and 60^o showed that the pickup ion temperature is the always the driver of instability and that any parallel drift velocity of the pickup ions is insufficient to excite a beam instability. An important consideration that was not included in this work is the nongyrotropy of the pickup ion distribution. In this study, we initialized the pickup ion population with a uniform spread in gyrophase angle, but this may not be appropriate. At Titan, the heavy ion gyroradii are of the same size as the atmospheric scale height, so finite larmor radius effects are present. Depending on where they are created relative to Titan, newborn ions can gyrate into Titan and be lost; those that are not lost can be detected by spacecraft but they will represent a more limited range of gyrophase angles. This effect was modeled by *Ledvina et al.* [2004]; *Ledvina and Cravens* [2005] using particle tracing in a steady-state global MHD model of the Titan interaction and explained analytically by *Hartle et al.* [2006a]; *Hartle and Sittler* [2007]. We chose not to include a nongyrotropic pickup ion distribution in this study because the degree of nongyrotropy of the pickup ions at Titan is not known, and a thorough study of the

behavior of nongyrotropic plasmas in the Titan environment is beyond the scope of this paper. Nongyrotropic distributions do not have a general linear theory and are capable of generating more types of wave modes than just the ion cyclotron waves, including coupled electromagnetic and electrostatic modes, depending on conditions [e.g. *Brinca et al.*, 1992; *Motschmann and Glassmeier*, 1993].

Finally, we want to point out that the results do not preclude the possibility that ion cyclotron waves have not been detected at Titan because they simply are not there. It is possible that turbulence throughout the mass-loading region or short time-scale variability in the orientation of the magnetic field and bulk plasma flow yields pickup ion populations that are not sufficiently anisotropic to generate waves or disrupts the waves in some other way that prevents them from being clearly observed. Testing these possibilities would require at two- or three-dimensional global simulation, which exist for Titan but have not yet been used to understand the lack of ion cyclotron wave generation there.

Acknowledgments. The authors wish to thank Dan Winske for helpful suggestions. This work was done in conjunction with the International Space Science Institute Working Group on Induced Magnetospheres. It was performed at Los Alamos National Laboratory under the auspices of the U.S. Department of Energy and was supported by the IGPP LANL mini-grant program and the NASA Cassini program.

References

Backes, H., F. M. Neubauer, M. K. Dougherty, N. Achilleos, N. Andre, C. S. Arridge, C. Bertucci, G. H. Jones, K. K. Khurana, C. T. Russell, and A. Wennmacher (2005), Titan's magnetic field signature during the first Cassini encounter, *Science*, *308*, 992–

995.

Bertucci, C. (2009), Characteristics and variability of Titan's magnetic environment, *Phil. Trans. R. Soc. A*, *367*, 789–798, doi:10.1098/rsta.2008.0250.

Bridge, H. S., J. W. Belcher, A. J. Lazarus, S. Olbert, J. D. Sullivan, F. Bagenal, and P. R. Gazis (1981), Plasma observations near Saturn: Initial results from Voyager 1, *Science*, *212*, 217–224.

Brinca, A. L., L. Borda del Agua, and D. Winske (1992), Nongyrotropy as a source of instability and mode coupling, *Geophys. Res. Lett.*, *19*(24), 2445–2448.

Coates, A. J. (2009), Interaction of Titan's ionosphere with Saturn's magnetosphere, *Phil. Trans. R. Soc. A*, *367*, 773–788.

Cowee, M. M., R. J. Strangeway, C. T. Russell, and D. Winske (2006), 1D hybrid simulations of planetary ion-pickup: Techniques and verification, *J. Geophys. Res.*, *111*(A12), A12213, doi:10.1029/2006JA011996.

Cowee, M. M., C. T. Russel, R. J. Strangeway, and X. Blanco-Cano (2007a), 1D hybrid simulations of obliquely propagating ion cyclotron waves: Application to ion pickup at Io, *J. Geophys. Res.*, *112*(A6), A06230, doi:10.1029/2006JA012230.

Cowee, M. M., D. Winske, C. T. Russell, and R. J. Strangeway (2007b), 1D hybrid simulations of planetary ion-pickup: Energy partition, *Geophys. Res. Lett.*, *34*, L02,113, doi:10.1029/2006GL028285.

Cowee, M. M., C. T. Russel, and R. J. Strangeway (2008), 1D hybrid simulations of planetary ion-pickup: effects of variable plasma and pickup conditions, *J Geophys Res*, *113*(A8), A08220, doi:10.1029/2008JA013066.

Frank, L. A., and W. Paterson (2000), Return to Io by the Galileo spacecraft: Plasma observations, *J. Geophys. Res.*, *105*(A11), 25,363–25,378.

Frank, L. A., W. R. Paterson, K. L. Ackerson, V. M. Vasyliunas, F. V. Coroniti, and S. J. Bolton (1996), Plasma observations at Io with the Galileo spacecraft, *Science*, *274*(5286), 394–395.

Gary, S. P., and C. D. Madland (1988), Electromagnetic ion instabilities in a cometary environment, *J. Geophys. Res.*, *93*(A1), 235–241.

Gary, S. P., and R. Sinha (1989), Electromagnetic waves and instabilities from cometary ion velocity shell distributions, *J. Geophys. Res.*, *94*(A7), 9131–9138.

Gary, S. P., and D. Winske (1993), Simulations of ion cyclotron anisotropy instabilities in the terrestrial magnetosheath, *J. Geophys. Res.*, *98*(A6), 9171–9179.

Gary, S. P., C. D. Madland, and B. T. Tsurutani (1985), Electromagnetic ion-beam instabilities .2., *Phys. Fluids*, *28*(12), 3691–3695.

Gary, S. P., C. D. Madland, D. Schriver, and D. Winske (1986), Computer simulations of electromagnetic cool ion beam instabilities, *J. Geophys. Res.*, *91*(A4), 4188–4200.

Gary, S. P., K. Akimoto, and D. Winske (1989), Computer simulations of cometary-ion/ion instabilities and wave growth, *J. Geophys. Res.*, *94*(A4), 3513–3525.

Hartle, R. E., and E. C. J. Sittler (2007), Pickup ion phase space distributions: Effects of atmospheric spatial gradients, *J. Geophys. Res.*, *112*, A07104, doi: 10.1029/2006JA012157.

Hartle, R. E., E. C. J. Sittler, K. W. Ogilvie, J. D. Scudder, A. J. Lazarus, and S. K. Atreya (1982), Titan's ion exosphere observed from Voyager 1, *J. Geophys. Res.*, *87*(A3), 1383–1394.

Hartle, R. E., E. C. J. Sittler, F. M. Neubauer, R. E. Johnson, H. T. Smith, F. J. Crary, D. J. McComas, D. Young, A. J. Coates, D. Simpson, S. Bolton, D. B. Reisenfeld, K. Szego, J. J. Berthelier, A. Rymer, J. Vippola, J. Steinberg, and N. Andre (2006a), Preliminary interpretation of Titan plasma interaction as observed by the Cassini Plasma Spectrometer: Comparisons with Voyager 1, *Geophys. Res. Lett.*, *33*, L08201, doi:10.1029/2005GL024817.

Hartle, R. E., E. C. Sittler, F. M. Neubauer, R. E. Johnson, H. T. Smith, F. J. Crary, D. J. McComas, D. Young, A. J. Coates, D. Simpson, S. Bolton, D. B. Reisenfeld, K. Szego, J. J. Berthelier, A. Rymer, J. Vilppola, J. Steinberg, and N. Andre (2006b), Initial interpretation of Titan plasma interaction as observed by the Cassini plasma spectrometer: Comparisons with Voyager 1, *Planet. Space Sci.*, *54*, 1211–1224.

Huddleston, D. E., R. J. Strangeway, J. Warnecke, C. T. Russell, M. G. Kivelson, and F. Bagenal (1997), Ion cyclotron waves in the Io torus during the Galileo encounter - warm plasma dispersion analysis, *Geophys. Res. Lett.*, *24*(17), 2143–2146.

Huddleston, D. E., R. J. Strangeway, J. Warnecke, C. T. Russell, and M. G. Kivelson (1998), Ion cyclotron waves in the Io torus: Wave dispersion, free energy analysis, and SO2+ source rate estimates, *J. Geophys. Res.*, *103*(E9), 19,887–19,889.

Johnson, R. E., H. T. Smith, O. J. Tucker, and M. Liu (2006), The Enceladus OH Tori at Saturn, *Astrophys. J.*, *644*, L137–139.

Khurana, K. K., M. K. Dougherty, C. T. Russell, and J. Leisner (2007), Mass loading of Saturn's magnetosphere near Enceladus, *J. Geophys. Res.*, *112*, A08203, doi: 10.1029/2006JA012110.

Kivelson, M. G. (1996), A magnetic signature at Io: Initial report form the Galileo magnetometer, *Science*, *274*(5285), 165–165.

Kivelson, M. G., K. K. Khurana, R. J. Walker, J. Warnecke, C. T. Russell, J. A. Linker, D. J. Southwood, and C. Polanskey (1996), Io's interaction with the plasma torus - Galileo magnetometer report, *Science*, *274*(5286), 396–398.

Le, G., X. Blanco-Cano, C. T. Russell, X. W. Zhou, F. Mozer, K. J. Trattner, S. A. Fuselier, and B. J. Anderson (2001), Electromagnetic ion cyclotron waves in the high-altitude cusp: Polar observations, *J. Geophys. Res.*, *106*(A9), 19,067–19,079.

Ledvina, S. A., and T. E. Cravens (2005), Ion distributions in Saturn's magnetosphere near Titan, *J. Geophys. Res.*, *110*, A06211, doi:10.1029/2004JA010771.

Ledvina, S. A., S. H. Brecht, and J. G. Luhmann (2004), Ion distributions of 14 amu pickup ions associated with Titan's plasma interaction, *Geophys. Res. Lett.*, *31*, L17S10, doi:10.1029/2004GL019861.

Leisner, J. S., C. T. Russell, M. K. Dougherty, X. Blanco-Cano, R. J. Strangeway, and C. Bertucci (2006), Ion cyclotron waves in Saturn's E ring: Initial Cassini observations, *Geophys. Res. Lett.*, *33*(11), L11,101.

Modolo, R., and G. Chanteur (2008), A global hybrid model for Titan's interaction with the Kronian plasma: Application to the Cassini Ta flyby, *J. Geophys. Res.*, *113*, A01,317, doi:10.1029/2007JA012453.

Motschmann, U., and K. H. Glassmeier (1993), Nongyrotropic distribution of pickup ions at comet P/Grigg-Skjellerup: a possible source of wave activity, *J. Geophys. Res.*, *98*(A12), 20,977–20,983.

Ness, N. F., M. Acuna, R. Lepping, J. E. P. Connerney, K. W. Behannon, and L. F. Burlaga (1981), Magnetic field studies by Voyager 1: Preliminary results at Saturn, *Science*, *212*, 211–217.

Omidi, N., and D. Winske (1986), Simulation of the solar wind interaction with the outer regions of the coma, *Geophys. Res. Lett.*, *13*(4), 397–400.

Russell, C. T., and M. G. Kivelson (2000), Detection of SO in Io's exosphere, *Science*, *287*, 1998–1999.

Russell, C. T., and M. G. Kivelson (2001), Evidence for sulfur dioxide, sulfur monoxide, and hydrogen sulfide in the Io exosphere, *J. Geophys. Res.*, *106*(E12), 33,267–33,272.

Russell, C. T., X. Blanco-Cano, Y. L. Wang, and M. G. Kivelson (2003a), Ion cyclotron waves at Io: Implications for the temporal variation of Io's atmosphere, *Planet. Space Sci.*, *51*(14-15), 937–944.

Russell, C. T., X. Blanco-Cano, and M. G. Kivelson (2003b), Ion cyclotron waves in Io's wake region, *Planet. Space Sci.*, *51*, 233–238.

Russell, C. T., S. M. Mayerberger, and X. Blanco-Cano (2006a), Proton cyclotron waves at Mars and Venus, *Adv. Space Res.*, *38*(4), 745–751.

Russell, C. T., J. Leisner, C. S. Arridge, M. K. Dougherty, and X. Blanco-Cano (2006b), Nature of magnetic fluctuations in Saturn's middle magnetosphere, *J. Geophys. Res.*, *111*(A12), A12205, doi:10.1029/2007JA011921.

Rymer, A., H. T. Smith, A. Wellbrock, A. J. Coates, and D. T. Young (2009), Discrete classification and electron energy spectra of Titan's varied magnetospheric environment, *Geophys. Res. Lett.*, *36*, L15109, doi:10.1029/2009GL039427.

Sillanpaa, I., E. Kallio, P. Janhunen, W. Schmidt, K. Mursula, J. Vilppola, and P. Tanskanen (2006), Hybrid simulation study of ion escape at Titan for different orbital positions, *Adv. Space Res.*, *38*, doi:10.1016/j.asr.2006.01.005.

Simon, S., G. Kleindienst, A. Boesswetter, T. Bagdonat, U. Motschmann, K. H. Glassmeier, J. Schuele, C. Bertucci, and M. K. Dougherty (2007), Hybrid simulation of Titan's magnetic field signature during the Cassini T9 flyby, *Geophys. Res. Lett.*, *34*, L24S08, doi:10.1029/2007GL029967.

Szego, K., Z. Bebesi, G. Erdos, L. Foldy, F. J. Crary, D. J. McComas, D. Young, S. Bolton, A. J. Coates, A. Rymer, R. E. Hartle, E. C. Sittler, D. B. Reisenfeld, J. J. Bethelier, R. E. Johnson, H. T. Smith, T. W. Hill, J. Vilppola, J. Steinberg, and N. Andre (2005), The global plasma environment of Titan as observed by Cassini Plasma Spectrometer during the first two close encounters with Titan, *Geophys. Res. Lett.*, *32*, L20S05, doi:10.1029/2005GL022646.

Tokar, R. L., R. E. Johnson, T. W. Hill, D. H. Pontius, W. S. Kurth, F. J. Crary, D. Young, M. F. Thomsen, D. B. Reisenfeld, A. J. Coates, G. R. Lewis, E. C. Sittler, and D. Gurnett (2006), The interaction of the atmosphere of Enceladus with Saturn's plasma, *Science*, *311*, 1409–1412.

Tokar, R. L., R. J. Wilson, R. E. Johnson, M. G. Henderson, M. F. Thomsen, M. M. Cowee, E. C. Sittler, D. Young, F. J. Crary, H. J. McAndrews, and H. T. Smith (2008), Cassini detection of water group pick-up ions in the Enceladus torus, *Geophys. Res. Lett.*, *35*, L14202, doi:10.1029/2008GL034749.

Tsurutani, B. T., D. E. Page, E. J. Smith, B. E. Goldstein, A. L. Brinca, R. M. Thorne, H. Matsumoto, I. G. Richardson, and T. R. Sanderson (1989), Low-frequency plasma

waves and ion pitch angle scattering at large distances (¿3.5x105 km) from Giacobini-Zinner: Interplanetary magnetic field and a dependences, *J. Geophys. Res.*, *94*(A1), 18–28.

Warnecke, J., M. G. Kivelson, K. K. Khurana, D. E. Huddleston, and C. T. Russell (1997), Ion cyclotron waves observed at Galileo's Io encounter - implications for neutral cloud distribution and plasma composition, *Geophys. Res. Lett.*, *24*(17), 2139–2142.

Wei, H. Y., C. Russell, A. Wellbrock, M. K. Dougherty, and A. J. Coates (2009), Plasma environment at Titan's orbit with Titan present and absent, *Geophys. Res. Lett.*, *36*, L23202, doi:10.1029/2009GL041048.

Winske, D., and N. Omidi (1992), Hybrid codes: Methods and applications, in *Computer space plasma physics: Simulation techniques and software*, edited by H. Matsumoto and Y. Omura, pp. 103–160, Terra Scientific Publishing Co., Tokyo.

Figure 1. PSD of observed waves during (left) a Cassini pass through the Extended Neutral Cloud and (right) a Galileo pass by Io. The local gyrofrequencies of the heavy pickup ions are indicated by the dahsed lines. From *Leisner et al.* [2006] and *Russell and Kivelson* [2001].

Figure 2. PSD of observed waves during the Cassini (left) T21 and (right) T23 passes by Titan. The local gyrofrequency of the $m = 16$ ion is indicated.

Figure 3. Schematic of the ion pickup process at Io. Newborn ions will form a ring distribution in velocity space with perpendicular velocity equal to the nominal pickup velocity of 57 km/s. Over time, the ring scatters to a more isotropic configuration. From *Huddleston et al.* [1998].

Figure 4. Cartoon of the Titan interaction. The mass-loading region is approximated as a cylinder and the simulation box convects with the bulk plasma flow from upstream to downstream of Titan, becoming mass-loaded. Over time, the pickup ions generate waves which could be seen by spacecraft downstream of Titan.

Figure 5. Time histories of fluctuating wave energy in the injection region for runs with $v_p = 100$ km/s and $L = 0.005$ ions/cc/s.

Figure 6. B_y along the simulation axis, z, at four times during the run with $v_p = 100$ km/s and $L = 0.005$ ions/cc/s.

Figure 7. $v_{\perp,1}$-$v_{\perp,2}$ space (top) and $v_{\perp,1}$-$v_{||}$ space (bottom) of the injected ions at four times during the run with $v_p = 100$ km/s and $L = 0.005$ ions/cc/s.

Figure 8. ω-k spectrum of simulated waves seen during the test run with $v_p = 100$ km/s and $L = 0.005$ ions/cc/s. The test run is done with injection throughout the simulation box and continuously during the run, for the purposes of better approximating what a spacecraft sitting at a fixed position downstream of Titan would see.

Figure 9. Power spectral density of simulated waves seen during the test run with $v_p = 100$ km/s and $L = 0.005$ ions/cc/s. The dotted line indicates the CH_4^+ gyrofrequency. The test run is done with injection throughout the simulation box and continuously during the run, for the purposes of better approximating what a spacecraft sitting at a fixed position downstream of Titan would see.

Figure 10. Dispersion solutions for the parameters listed in Table 1 with a pickup ion ring with $T_\perp/T_{||} \sim 300$ (i.e. the ring has undergone some scattering from its initial $T_{||} \sim 0$ configuration).

Figure 11. Wave amplitudes at $\Omega_i t = 5.5$ for runs with varying injection rate, L, and $v_p = 100$, 70, and 40 km/s.

Figure 12. Power spectral density of simulated waves seen during the test run with $\alpha = 30^o$. The dotted line indicates the CH_4^+ gyrofrequency.

Table 1. Simulation Input Parameters

component	m	n	$T_\parallel$	$T_\perp$	v_p	L
	(m_p)	(/cc)	(eV)	(eV)	(km/s)	(/cc/s)
H^+ background	1	0.25	200	200	-	-
H_2^+ background	2	0.25	200	200	-	-
CH_4^+ pickup	16	-	$\sim$0	-	100	0.0007 - 0.0070
					70	0.0010 - 0.0184
					40	0.0041 - 0.1734

Total ion density at start of simulation is $0.5/cc$ and B_0 is 6 nT. Normalization: $v_A = 185$ km/s, $c/\omega_{pi} = 322$ km, $\Omega_i^{-1}/(2\pi) = 175$ s.

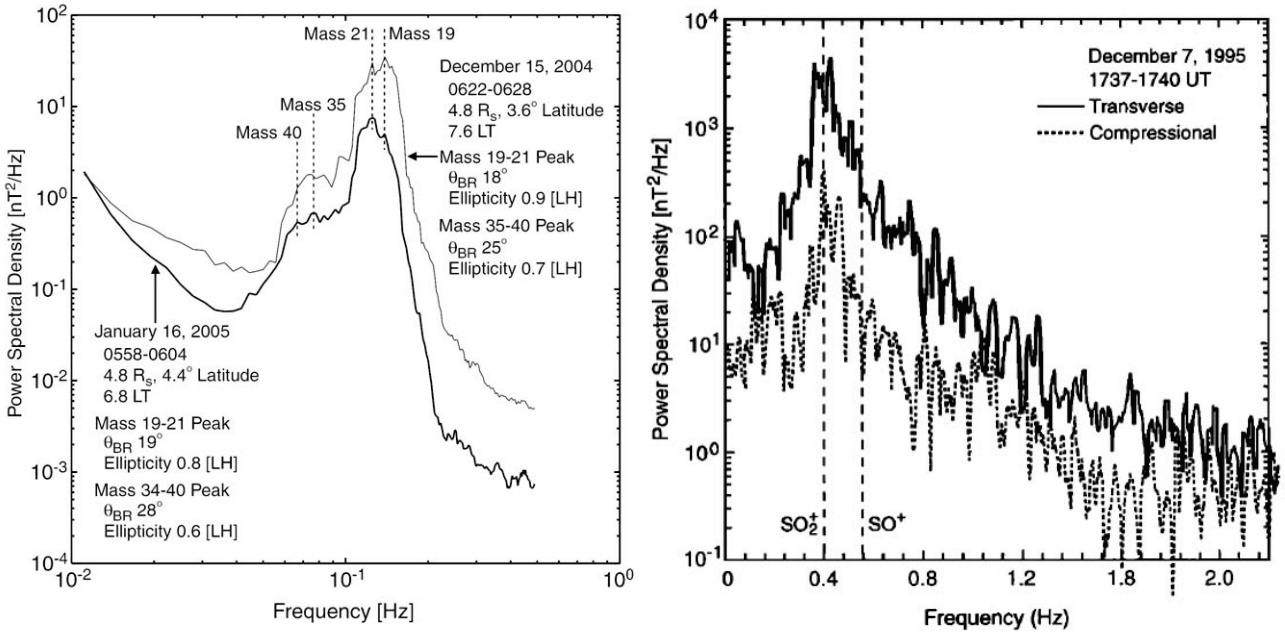

Figure 1. PSD of observed waves during (left) a Cassini pass through the Extended Neutral Cloud and (right) a Galileo pass by Io. The local gyrofrequencies of the heavy pickup ions are indicated by the dahsed lines. From *Leisner et al.* [2006] and *Russell and Kivelson* [2001].

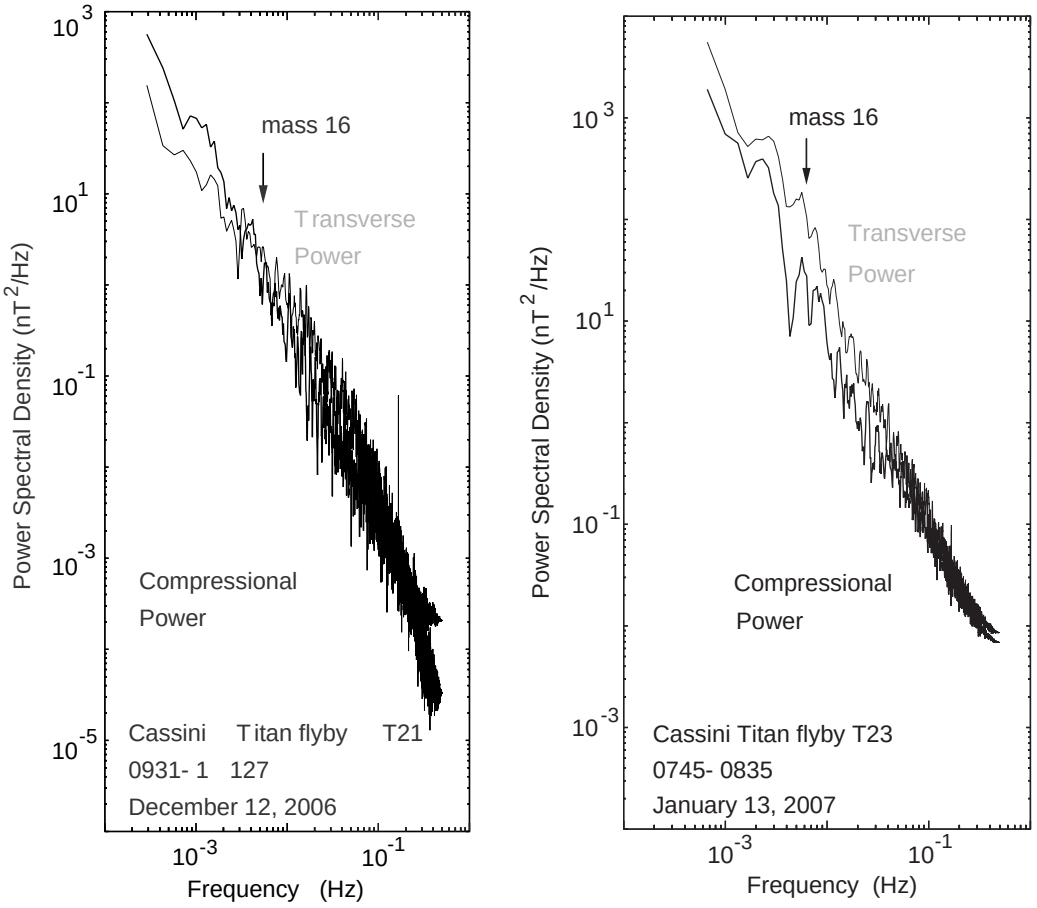

Figure 2. PSD of observed waves during the Cassini (left) T21 and (right) T23 passes by Titan. The local gyrofrequency of the $m = 16$ ion is indicated.

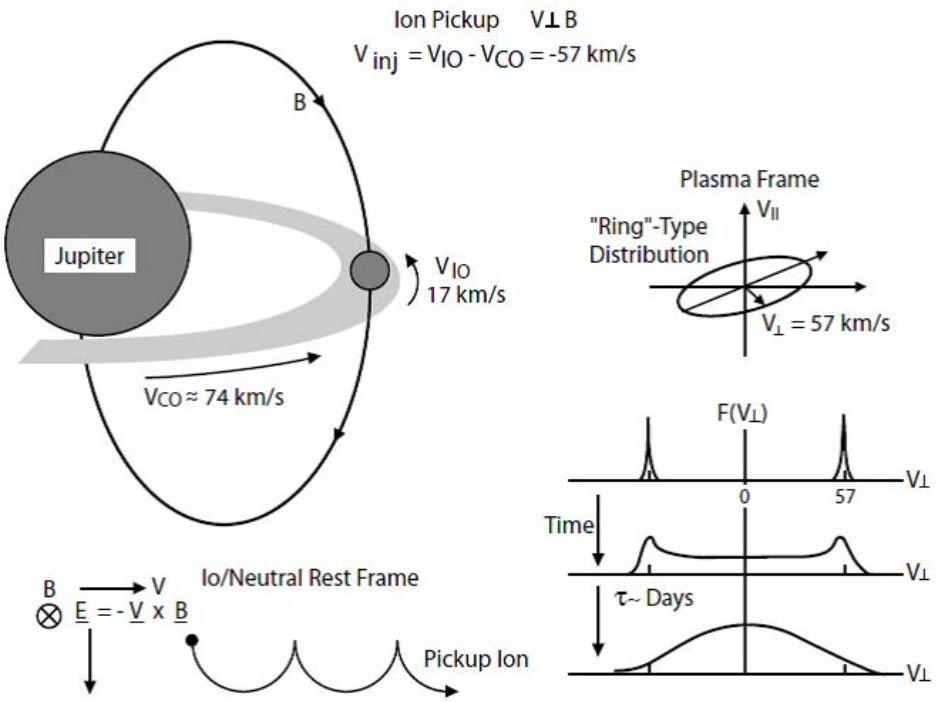

Figure 3. Schematic of the ion pickup process at Io. Newborn ions will form a ring distribution in velocity space with perpendicular velocity equal to the nominal pickup velocity of 57 km/s. Over time, the ring scatters to a more isotropic configuration. From *Huddleston et al.* [1998].

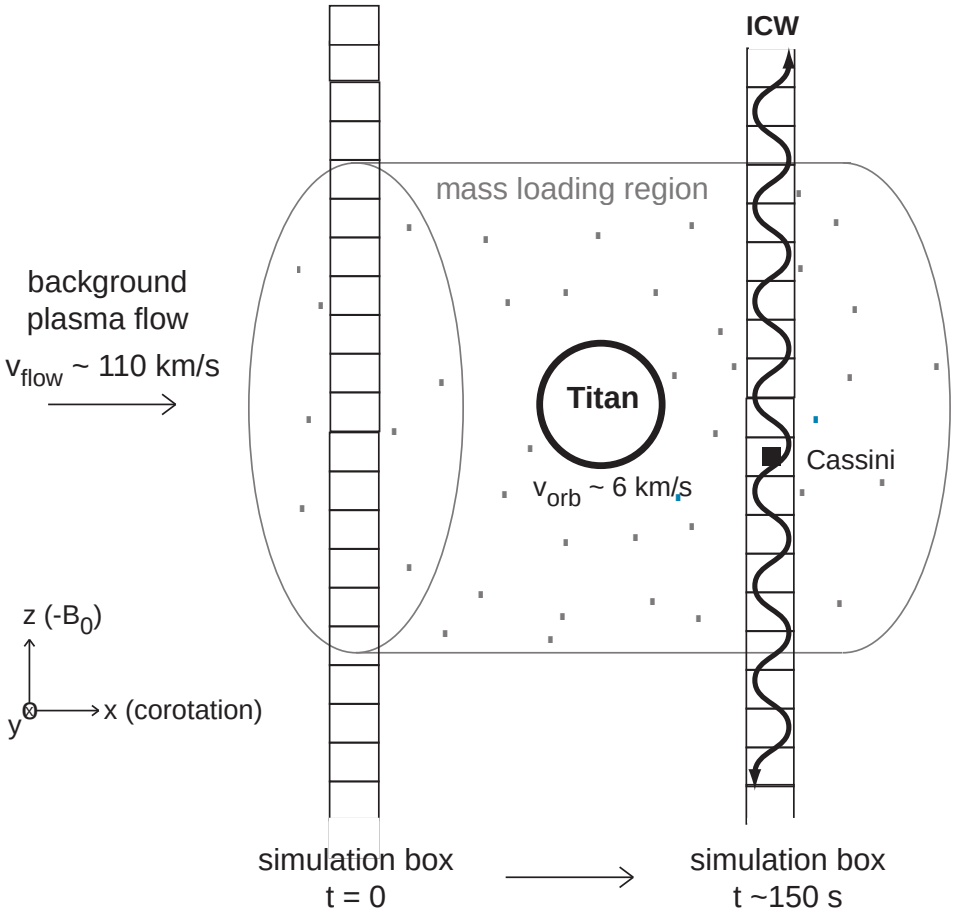

Figure 4. Cartoon of the Titan interaction. The mass-loading region is approximated as a cylinder and the simulation box convects with the bulk plasma flow from upstream to downstream of Titan, becoming mass-loaded. Over time, the pickup ions generate waves which could be seen by spacecraft downstream of Titan.

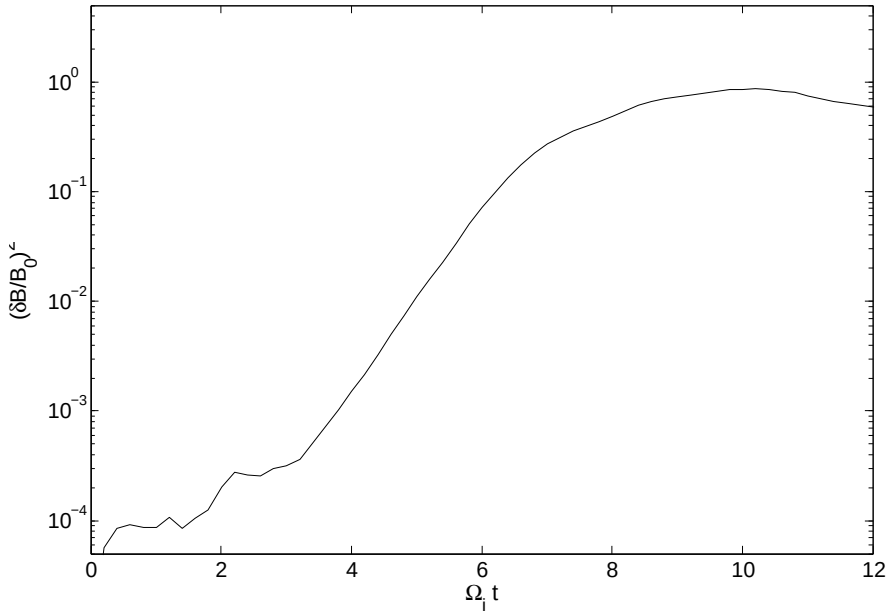

Figure 5. Time histories of fluctuating wave energy in the injection region for runs with $v_p = 100$ km/s and $L = 0.005$ ions/cc/s.

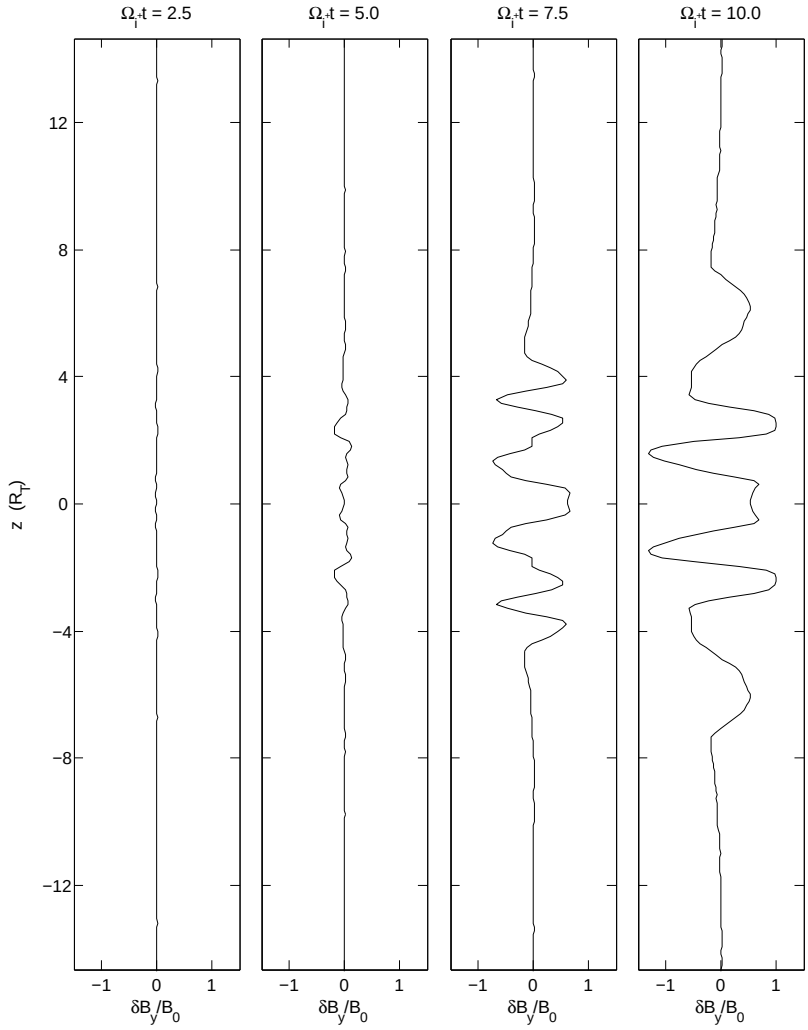

Figure 6. B_y along the simulation axis, z, at four times during the run with $v_p = 100$ km/s and $L = 0.005$ ions/cc/s.

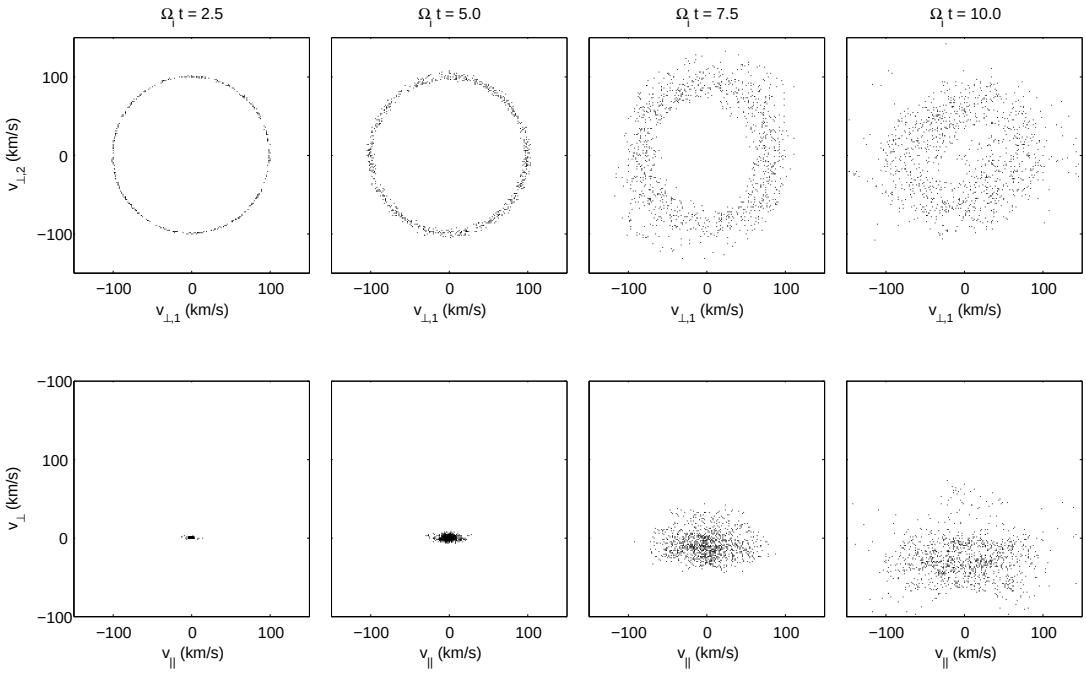

Figure 7. $v_{\perp,1}$-$v_{\perp,2}$ space (top) and $v_{\perp,1}$-$v_{||}$ space (bottom) of the injected ions at four times during the run with $v_p = 100$ km/s and $L = 0.005$ ions/cc/s.

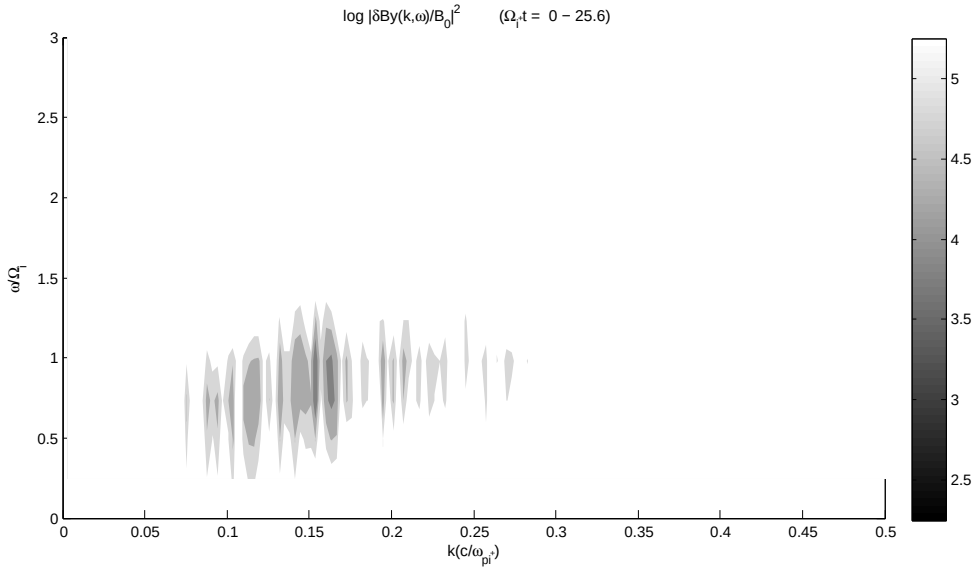

Figure 8. ω-k spectrum of simulated waves seen during the test run with $v_p = 100$ km/s and $L = 0.005$ ions/cc/s. The test run is done with injection throughout the simulation box and continuously during the run, for the purposes of better approximating what a spacecraft sitting at a fixed position downstream of Titan would see.

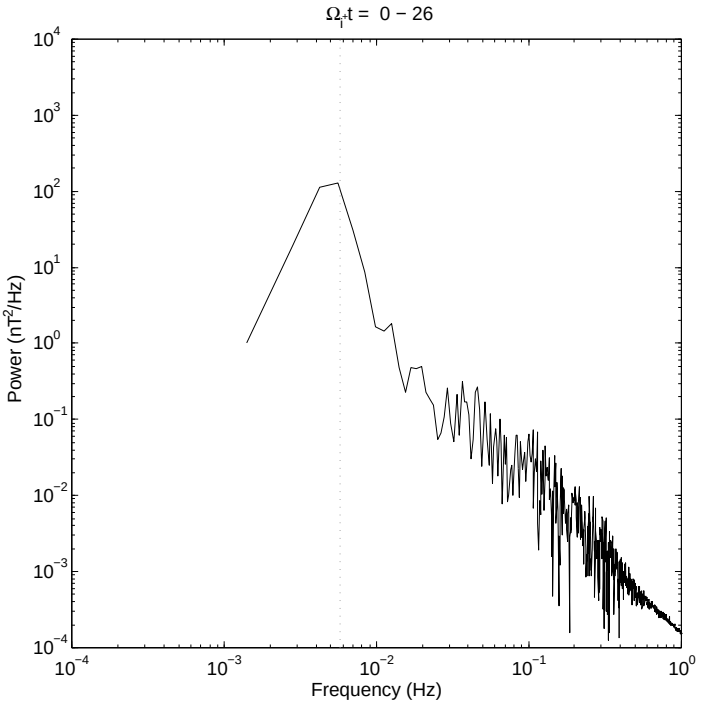

Figure 9. Power spectral density of simulated waves seen during the test run with $v_p = 100$ km/s and $L = 0.005$ ions/cc/s. The dotted line indicates the CH_4^+ gyrofrequency. The test run is done with injection throughout the simulation box and continuously during the run, for the purposes of better approximating what a spacecraft sitting at a fixed position downstream of Titan would see.

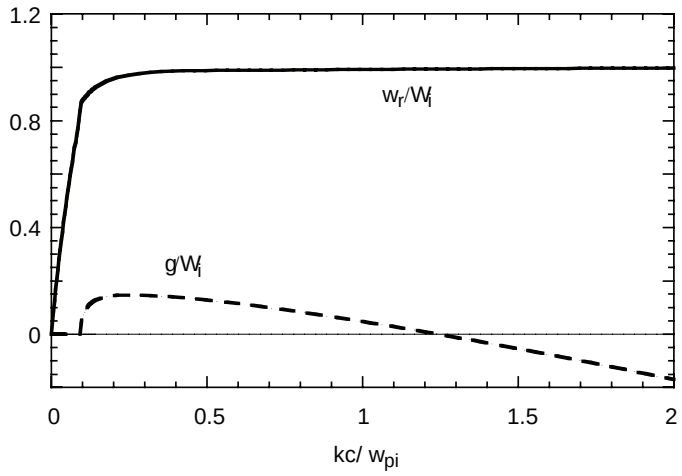

Figure 10. Dispersion solutions for the parameters listed in Table 1 with a pickup ion ring with $T_\perp/T_{||} \sim 300$ (i.e. the ring has undergone some scattering from its initial $T_{||} \sim 0$ configuration).

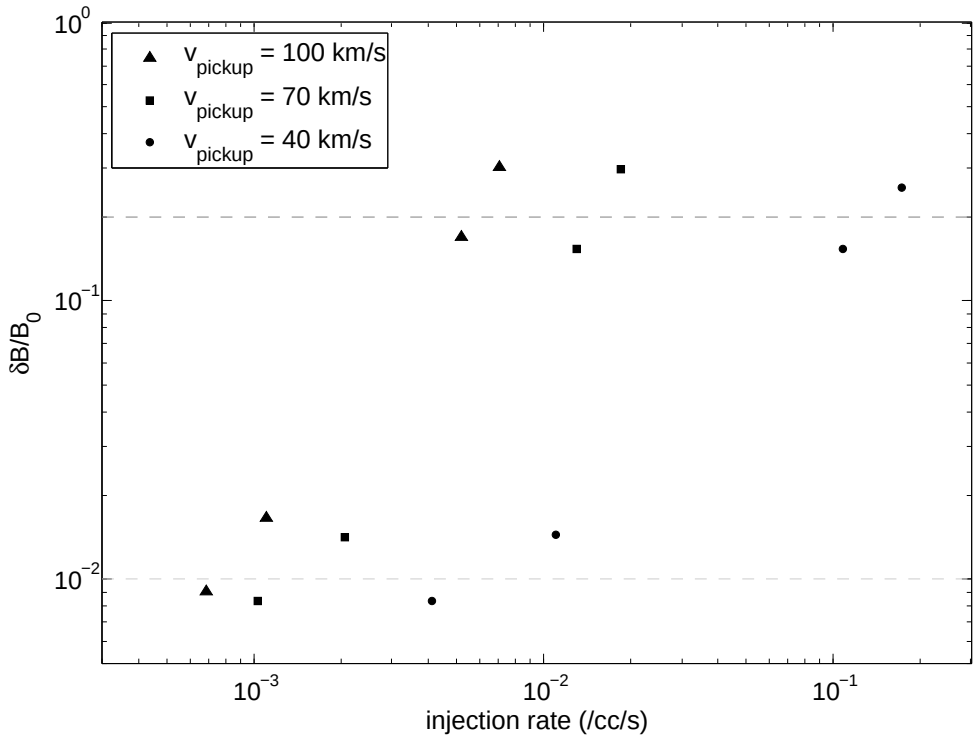

Figure 11. Wave amplitudes at $\Omega_i t = 5.5$ for runs with varying injection rate, L, and $v_p = 100$, 70, and 40 km/s.

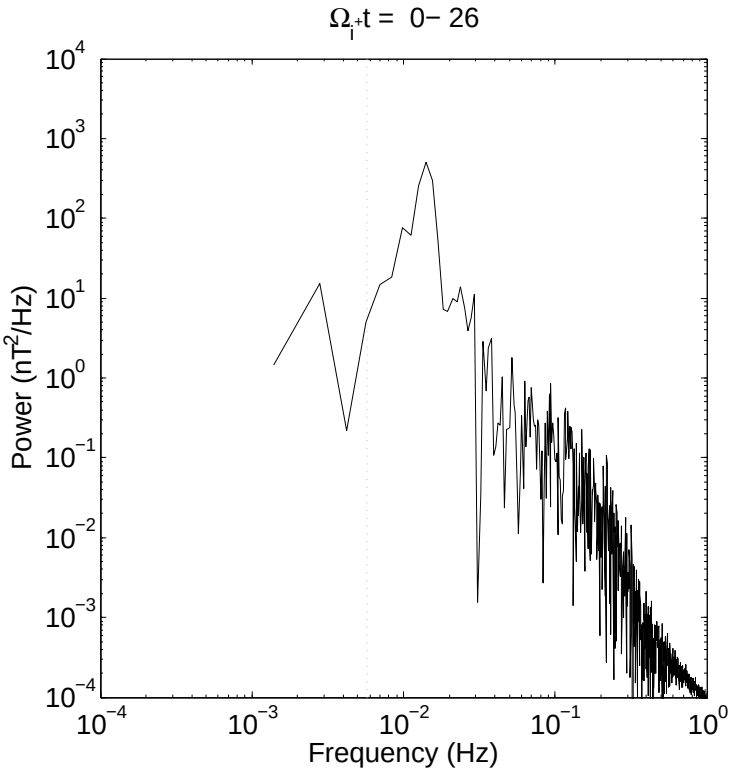

Figure 12. Power spectral density of simulated waves seen during the test run with $\alpha = 30^o$. The dotted line indicates the CH_4^+ gyrofrequency.